Kinetic Solvent Effects in Organic Reactions

Belinda L. Slakman and Richard H. West*

Department of Chemical Engineering, Northeastern University, Boston MA.
*Corresponding author: r.west@northeastern.edu

Abstract

This article reviews prior work studying reaction kinetics in solution, with the goal of using this information to improve detailed kinetic modeling in the solvent phase. Both experimental and computational methods for calculating reaction rates in liquids are reviewed. Previous studies, which used such methods to determine solvent effects, are then analyzed based on reaction family. Many of these studies correlate kinetic solvent effect with one or more solvent parameters or properties of reacting species, but it is not always possible, and investigations are usually done on too few reactions and solvents to truly generalize. From these studies, we present suggestions on how best to use data to generalize solvent effects for many different reaction types in a high throughput manner.

Lead-in

Several environmentally, medically, and industrially relevant chemical systems involve liquid-phase reactions, including secondary organic aerosol formation, oxidation of fuels in the condensed phase, and radical scavenging in the body [1–3]. Learning about complex systems requires knowledge of solvent effects on the rates of elementary chemical reactions, many of which are radical-molecule and radical-radical reactions. Depending on the solvent, rates of reaction can vary by orders of magnitude, thus changing likely pathways and product distributions. Furthermore, knowledge of kinetic solvent effects not only helps with generation of liquid-phase reaction mechanisms, but can aid in the design of solvents to promote a desired reaction pathway or product [4].

1   Introduction

Predicting the rates of chemical reactions occurring in solution, particularly in the absence of experimental data, is a challenging task. However, common families of reactions occur in both the liquid-phase and gas-phase; for example, gas-phase combustion of hydrocarbon fuels will be dominated by hydrogen abstraction reactions, as will the low temperature, liquid-phase oxidation of fuels by exposure to the atmosphere. Since these reaction types also occur in the gas phase and are sometimes better studied, it can be advantageous to modify these known gas phase reaction rates rather than predicting the solution phase kinetics directly.

One example of how presence of a solvent modifies effective reaction rate, k_{eff}, is due to the solvent's physical diffusion limitation:

$$\frac{1}{k_{\text{eff}}} = \frac{1}{k_{\text{diff}}} + \frac{1}{k_{\text{int}}} \tag{1}$$

where k_{diff} is the rate of diffusion and k_{int} is the intrinsic rate of reaction, not accounting for diffusion. The rate of diffusion is proportional to the sum of the radii R and sum of the diffusivities D of the reacting species[5]:

$$k_{\text{diff}} = 4\pi R D \tag{2}$$

The diffusivity of a species A, D_A, can be estimated using the Stokes-Einstein relation:

$$D_A = \frac{k_{\text{B}} T}{6 \pi \eta r_A} \tag{3}$$

where k_{B} is the Boltzmann's constant, T is temperature, η is the solvent viscosity, and r_A is the radius of chemical species A.

As diffusion corrections to modify gas-phase reaction rate are already known (see ref. 6), this review focuses on the intrinsic solvent effect on chemical reaction rates. As opposed to the physical diffusion effect, the intrinsic effect accounts for changes in the chemical environment of reactants and transition state, and modifies the reaction barrier (see Figure 1)[7].

Solvent effects on the reaction rate depend on both the nature of the solvent and the type of reaction occurring, and thus can be challenging to apply systematically. It is helpful to consider previous work in this field in order to understand and ultimately generalize solvent effects.
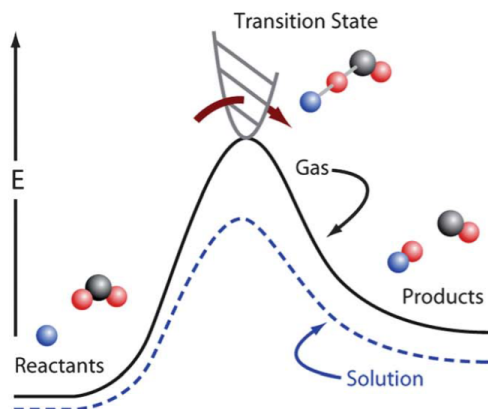
Figure 1: Example of a potential energy surface for a reaction in gas-phase (black) and in solution (blue). A solvent may have different stabilization effects on the reactants, transition states, and products in a chemical reaction. Reproduced from ref. 7 with permission of The Royal Society of Chemistry.

In Figure 1, it is assumed that the solvent does not participate in the reaction via atom bonding or transfer, and only provides electrostatic interactions which modify the solution phase energy of the reactants, transition state, and products. In reality, there are situations where the solvent does participate, thus changing the reaction mechanism; for example, Liang et al. show that water can assist a 1,2 hydrogen shift step in a cycloaddition mechanism to form heterocycles[8]. While consideration of these alternative steps are important in determining overall reaction mechanism and kinetics, we will mainly consider those cases in which the solvent does not participate in the reaction, to simplify the goal of generalizing the effect solvation has on gas phase rates.

Towards this goal, sections 2 and 3 describe experimental and theoretical approaches, respectively, used to study intrinsic solvent effects. Section 4 then describes previous solvent effect discoveries organized by reaction family. Section 5 concludes with a perspective on how to best understand these solvent effects, and a suggestion to leverage data to generalize solvent effects for different types of chemical reactions.

3

2 Experimental techniques for determining reaction rates in liquids

To better understand kinetic solvent effects on chemical reactions, experiments aim to measure reaction rates in a variety of solvents. Experimentally determining reaction rates for radical reactions in solution can be difficult due to the short-lived nature of some radicals; however, some methods have been developed over the last century and are commonly used for measuring these kinetics. In an early method pioneered by Briers and Chapman known as rotating sector, or the intermittent-illumination method (IIM), a sample is exposed to a constant intensity of light for intermittent periods of time, such that the amount of time spent in light and in the dark remains constant [9–11]. The average reaction rate, $\overline{W_M}$, can be calculated by:
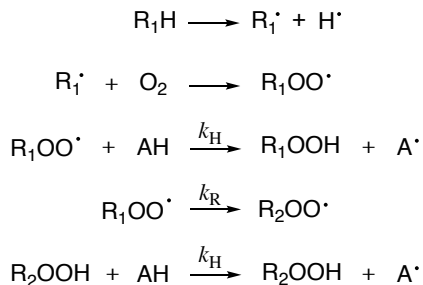
$$\overline{W_M} = \frac{k_p}{\sqrt{2k_t}}[M]\sqrt{\phi I}(1+r)^{-1} \tag{4}$$

where k_p and k_t are the propagation and termination rates, respectively, $[M]$ is the concentration of the compound under investigation, M, reacting with a radical, ϕ is the quantum yield of photoinitiation, I is the light intensity, and r is the ratio of time in the dark to time in the light [11]. This method has been applied to reactions in gas phase and solution, including polymerization and radical recombination [12–14]. This method, however, can only be used for some specific types of radical chain reactions, with one requirement being that they can be photochemically initiated [15].

A very common method for measuring the reaction rate of radical reactions in both gas and liquid-phase is laser flash photolysis. In this method a sample is excited by a pulse from a laser, and radical species are monitored by measurement of their spectral absorption. The spectral absorption can be measured with electron spin resonance, in which the unpaired electron of the radical interacts with the nuclei in the molecule leading to a mapping of electron density [16].

An indirect way of measuring the rate constants for radical-molecule reactions is the radical clock method, which uses a known unimolecular reaction rate and a measured product distribution to determine an unknown radical-molecule reaction rate [15]. For example, Roschek and co-workers developed radical clocks for peroxyl radical reactions using the competition between a unimolecular rearrangement of a peroxyl radical ($R_1OO \cdot \longrightarrow R_2OO$, k_R)

and a bimolecular H-atom transfer $(\text{ROO}\cdot + \text{AH} \longrightarrow \text{ROOH} + \text{A}\cdot, k_H)$[17]. This concept is shown in Figure 2.

$$\text{R}_1\text{H} \longrightarrow \text{R}_1\overset{\cdot}{} + \text{H}^{\cdot}$$

$$\text{R}_1^{\cdot} + \text{O}_2 \longrightarrow \text{R}_1\text{OO}^{\cdot}$$

$$\text{R}_1\text{OO}^{\cdot} + \text{AH} \xrightarrow{k_\text{H}} \text{R}_1\text{OOH} + \text{A}^{\cdot}$$

$$\text{R}_1\text{OO}^{\cdot} \xrightarrow{k_\text{R}} \text{R}_2\text{OO}^{\cdot}$$

$$\text{R}_2\text{OOH} + \text{AH} \xrightarrow{k_\text{H}} \text{R}_2\text{OOH} + \text{A}^{\cdot}$$

$$\boxed{k_H = \frac{k_R[\text{R}_2\text{OOH}]}{[\text{R}_1\text{OOH}][\text{AH}]}}$$

Figure 2: Concept of peroxyl radical clock for predicting unknown k_H from known k_R[17].

Jha and Pratt point out some limitations to the structure of the "clock" or initial molecule used, R_1H[18]. If $\text{R}_1\cdot$ is either persistent or highly stabilized, it cannot carry the chain reaction, and a large concentration of substrate is required. They describe a modification the radical clock method using peroxyesters, making it possible to study a wider range of reactions.

3   Computational chemistry methods for determining solvent effect

Computational chemistry provides an alternate approach to experiments for determining intrinsic kinetic solvent effects. Reaction rates $k(T)$ can be calculated directly using classical transition state theory[19]:

$$k(T) = \frac{k_B T}{h} \exp\left(\frac{-\Delta G^{\ddagger}}{RT}\right) \tag{5}$$

where k_B represents the Boltzmann's constant, T is temperature, h is Planck's constant, R is the ideal gas constant, and $\Delta G^{\ddagger}$ is the difference in Gibbs free energy between transition state and reactant. Transition state theory requires the properties of the reactants and transition states of a reaction to

be known or calculated using quantum chemistry, specifically by solving the Schrödinger equation for each of these chemical species:

$$\hat{H}\psi = E\psi \tag{6}$$

where $\hat{H}$ is the Hamiltonian operator, ψ is the system's wave function, and E is the total energy of a chemical species. Depending on the size of the system, E is not trivial to calculate and some approximations to the Schrödinger equation are made to be able to solve it numerically, to be discussed in Section 3.1

Once a species' energy is known, intrinsic solvent effect can then be determined. The differential solvation between reactants and transition states causes a energetic change between these two species, modifying $\Delta G^{\ddagger}$ when changing phases and thus affecting the reaction rate as indicated in equation (5) and illustrated in Fig. 1. Several computational methods are commonly utilized for obtaining geometries of reactants and transition states, and their properties, i.e. electronic energies and frequencies.

3.1   Density functional theory

One popular set of methods used to approximately obtain the electronic structures of molecules, radicals, and activated complexes (transition states) is based on density functional theory (DFT). DFT considers electron density and electronic energy rather than the wave function[20,21]. The specific DFT method chosen has an impact on the accuracy of chemical species' geometries and energies, and it was previously found that the accuracy of density functionals for predicting barrier height is correlated with their accuracy for transition state geometries[22]. The approximate functionals which are used in DFT predict the transition state energies too low because they incorrectly delocalize electrons[23]. However, when comparing both reactants and transition states in gas and liquid, this discrepancy matters less since it will be present in both phases, and some cancellation of error will occur. Because of this cancellation of error, when DFT is used to compute solvent effects, comparison to experimental rates has shown that it provides sufficient accuracy to capture the desired effects[24,25].
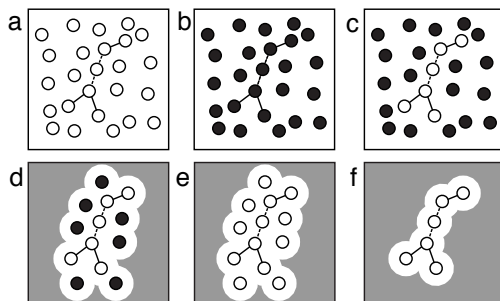
Figure 3: Discrete (a-c), hybrid (d-e), and continuum (f) models of solvation, for calculating properties of chemical species in solution in order to determine reaction rate. White circles represent atoms treated with QM whereas black circles correspond to MM treatment. The grey represents a polarizable or conducting continuum.

3.2   Solvation models

The next challenge to computational calculation of solvent effects is the representation of the solvent and how its presence affects the energy of chemical species. Computational methods for estimating solvation energies are reviewed in[26] and are depicted in Figure 3. They generally fall into two categories: those that represent solute and solvent molecules explicitly (Figures 3a-c), and those that represent only solute molecules explicitly and the solvent molecules somewhere in between explicit and implicit (Figures 3d-f). Explicit treatment is done either quantum mechanically (QM) (Figure 3a), with molecular mechanics (MM) (Figure 3b), or some combination of both, as in QM/MM (Figure 3c).

Continuum solvation models represent solvation as a solute placed inside a cavity within an implicit solvent, which is modeled as a continuum with a constant property such as conductivity or dielectric constant (Figure 3f). The solute cavity can be shaped like a sphere or ellipsoid, or as in more modern methods, based upon a superposition of atom-centered spheres[27]. However, representing a solvent this way does not account for local solute-solvent interactions, and the assumption that the dielectric constant near the solute surface is equal to the bulk dielectric constant is inaccurate.

One such continuum solvation method is known as the Conductor-like Screening Model (COSMO), and allows the solute cavity to be arbitrarily

shaped[28–30]. The method makes calculation of analytical gradients more efficient and geometry optimization can be done faster and more realistically[28]. COSMO-RS is an updating of COSMO for "real solvents", that is, without assumption of dielectric screening theory, which does not hold for very polar solvents[29,30]. COSMO-RS relies on viewing molecular interactions locally, through pairwise interactions, rather than considering ensembles of molecules interacting electrostatically and through van der Waals forces.

The shells theory proposed by Pliego is an example of a hybrid implicit/explicit solvation method[31]. In this solvation treatment, the solvent shell closest to the solute (S_1), representing solute-solvent interaction, is treated either fully quantum mechanically, as in Figure 3e, or with molecular dynamics based on classical force fields, as in Figure 3d. The remaining solvent, S_2, is treated with continuum solvation. When the number of solvent molecules in S_1 becomes infinite, this theory converges to the full discrete solvent representation. This approach is also known as the cluster-continuum model, mixed discrete-continuum model, or quasichemical theory[27].

A recommended method for calculating liquid-phase free energies is SMD[32]. It is a continuum method but takes into account contributions from the first solvation shell via paremetrization. This model, like its authors' other SM_x methods, includes a term for non-electrostatic effects due to cavity formation, dispersion interactions, and solvent structure. The contribution is dependent upon the solvent-accessible surface area (SASA) of each solute atom. The main feature distinguishing SMD from the other SM_x methods is that it utilizes a continuous charge density of the solute, rather than a discrete representation. In the Gaussian computational chemistry program[33], the method is combined with the polarizable continuum method (PCM)[34] for single-point energy calculations on a solute in a solvent. However, it can be used with other algorithms such as COSMO[28] and COSab[35] implemented in other software packages.

A recent method developed by Pomogaeva and Chipman[36], known as the composite method for implicit representation of solvent (CMIRS), uses six parameters to describe interactions between solute and solvent including dispersion, exchange, hydrogen bonding, and long range electrostatic interactions. Because of low level of parameterization, this model is believed to capture a higher level of physical truth than other highly parameterized solvation models[36]. For hydration energy, the mean unsigned error (MUE) may be as low as 0.8 kcal/mol for neutral solutes and 2.4 kcal/mol for ionic solutes, and has been parametrized for the B3LYP and Hartree-Fock quantum chemistry

methods[36]. With regards to solvation kinetics, Silva et al. parametrized the CMIRS model for methanol in order to predict activation free energy barriers for S_N2 and S_NAr reactions[37]. Both CMIRS and SMD were compared to experimental data of solvation free energies and while they perform similarly for neutral species, the MUE for CMIRS is lower in the case of anion and cation solutes. For free energy barriers, CMIRS performs similarly to COSMO-RS while SMD is slightly worse[37].

4 Kinetic solvent effects within reaction families

Kinetic solvent effects are usually most generalizable within a particular type or family of reaction, and the following section will be organized accordingly. However, as will be shown in several studies, the kinetic solvent effect can vary within a reaction family and across solvents.

4.1 Hydrogen abstraction

The largest body of literature on solvent effects on reaction rates is in bimolecular hydrogen abstraction reactions. Nearly four decades ago, Das et al. used laser flash photolysis to study the reaction of tert-butoxyl radicals with phenols in six solvents[39]. The rate decreased in polar solvents, explained by the capability of the phenolic OH group to hydrogen bond with solvent molecules. Ingold and co-workers have attempted since to further deduce these solvent effects in hydrogen abstraction reactions. Valgimigli et al. found that the solvent effect on abstraction of the phenolic hydrogen from α-tocopherol by both tert-butoxyl radical and 2,2,-diphenyl-1-picrylhydrazyl (DPPH·) is independent of the *radical* in almost every solvent they tested[38] (see Figure 4). This result is especially surprising, since for these two radicals, the reaction rate in the same solvent differs by over 10^6. Any deviation from this behavior, as in tert-butyl alcohol, is thought to be due to the reaction being partially diffusion controlled. The reaction of α-tocopherol with tert-butoxyl was further investigated in four solvents; the rate constant decreased with increasing β_2^H value[40], a measure of solvent basicity.

In solvents with both high dielectric constant and basicity, different behavior is observed, discovered in a study of the reaction between Trolox and
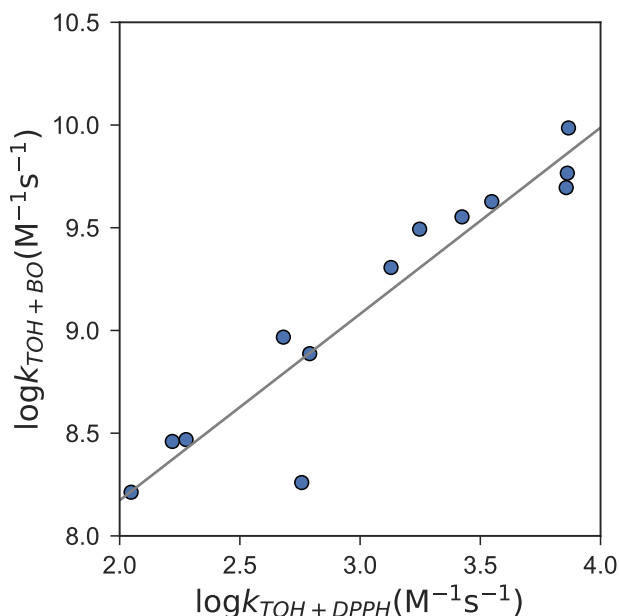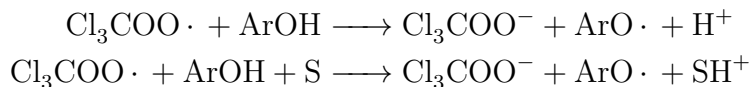
Figure 4: The solvent effect on hydrogen abstraction from α-tocopherol is independent of the radical (DPPH (x-axis) or TOH (y-axis)). Each point represents a different solvent. Data from[38]

$Cl_3COO\cdot$[41]. In these solvents, a mechanistic shift from hydrogen atom abstraction to electron transfer occurs. This electron transfer mechanism may also be accompanied by a solvent-assisted proton loss, known as sequential proton loss electron transfer (SPLET):

$$Cl_3COO\cdot + ArOH \longrightarrow Cl_3COO^- + ArO\cdot + H^+$$
$$Cl_3COO\cdot + ArOH + S \longrightarrow Cl_3COO^- + ArO\cdot + SH^+$$

Thus, the electron transfer mechanism can account for rates which are higher than the rate one might expect by simply correlating rate with one solvent property. Foti et al. also discovered this fast electron-transfer reaction between phenols and DPPH[42]. While hydrogen atom transfer was dominant in nonpolar solvents most of the time, electron transfer still occurred if the radical was strongly oxidizing, as with $Cl_3COO\cdot$. Reactions proceeding via the electron-transfer mechanism should be faster in polar solvents.

But surprisingly, the rate constant was higher in ethanol than methanol despite methanol having a higher dielectric constant; the study attributed this inconsistency to solvent impurities.

The Snelgrove-Ingold correlation for hydrogen abstraction reactions relates the difference in rate constant between the reaction in gas and in solvent to the solvent's hydrogen bonding parameters α_2^H and β_2^H [43]:

$$\log_{10} \frac{k_{gas}}{k_{solvent}} = 8.3\alpha_2^H \beta_2^H. \tag{7}$$

Later, it was found that this single empirical equation could not describe an entire reaction family [44–46]. In solvents which support ionization, some hydrogen abstraction reactions, for example that of 2,2'-methylene-bis(4-methyl-6-*tert*-butylphenol) (BIS) with DPPH·, proceeded by the SPLET mechanism [46]. This led to a reaction which is zero-order in DPPH·. Because this is not true for the reactions of all phenols with DPPH·, it was suggested that properties of the reacting phenol play a role. One such property is the intramolecular H-bond in BIS, which may slow the reverse proton-transfer reaction, thus leading to the unusual effect observed. Furthermore, Nielsen and Ingold found that the β_2^H scale does not account for solvents' anion solvating properties, and thus reactions involving proton transfer do not quite follow the Snelgrove-Ingold correlation [47]. The Taft β scale [48] gives better correlations for these proton transfer reactions.

An experimental study by Warren and Mayer also note the failure of the generalized Snelgrove-Ingold correlation. They studied the effect of small amounts of solvent additives on the oxidation of ascorbate (vitamin C) by TEMPO radical. Their results indicate that solvent effect on hydrogen abstraction reactions is better explained by local solvent effects, as the effects are much greater than can be explained by bulk solvent properties [49].

In some types of hydrogen abstraction reactions, the effect of changing the solvent is low. The reaction between ascorbate and 2,2,6,6-tetramethylpiperidine-1-oxyl radical was studied experimentally [50]. The mechanism was best explained by proton-coupled electron transfer (PCET) (Figure 5), where an electron and proton are transferred simultaneously but between different sets of orbitals. This mechanism differs from SPLET, as the electron and proton are transferred in a single elementary step rather than sequentially. The solvent was varied between water and mixtures of water and dioxane, decreasing its polarity. The quantity investigated was the kinetic isotope effect (KIE), which is defined as the ratio of the rates of hydrogen abstraction in water
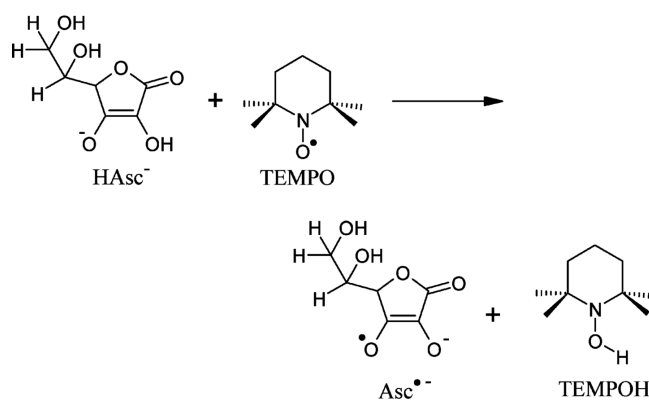
11

Figure 5: Example of the PCET mechanism for the hydrogen abstraction reaction between ascorbate and TEMPO radical[50]. Reprinted with permission from Sajenko, I., Pilepić, V., Brala, C. J., & Ursić, S. (2010). Solvent dependence of the kinetic isotope effect in the reaction of ascorbate with the 2,2,6,6-tetramethylpiperidine-1-oxyl radical: tunnelling in a small molecule reaction. The Journal of Physical Chemistry A, 114(10), 3423–3430. http://doi.org/10.1021/jp911086n. Copyright 2010 American Chemical Society.

and in D_2O. KIE was found to only slightly increase with decreasing solvent polarity. Interestingly, hydrogen tunneling was suspected to take place in all solvents studied, because the experimental KIEs were larger than expected.

From these studies it has generally been understood that solvent effects on hydrogen abstraction reactions are significant when looking at O-H bond abstraction, primarily because of the O-H bond's ability to participate in hydrogen bonding networks, but that the effect on C-H bond abstraction is negligible. Despite this assumption, Koner and co-workers generalized these effects to C-H and Sn-H bonds[51]. They explain the results as a stabilization of the abstracting species in polar solvents, rather than the hydrogen donor (which is the case for abstraction from the O-H bond). Thus, the nature of the abstracting species has a large effect on the reaction rate in solvents. They still hypothesize that the reaction of a non-polar hydrogen donor and non-polar abstracting radical will have little solvent effect, but acknowledge this is hard to test experimentally due to the high activation barrier of these reactions.

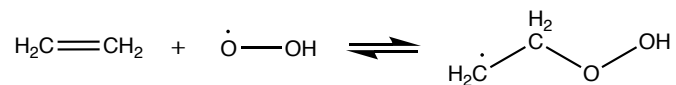## 4.2   Radical addition to multiple bonds

Figure 6:   Example of a radical addition to multiple bond reaction: Addition of hydroperoxyl radical to ethane.

Kinetic solvent effects on the addition of radicals to multiple bonds (Figure 6) has mainly been investigated theoretically and has been extensively studied by the groups of Fouassier[52–54] and Radom[55–58]. In one such study, when various radicals were added to methyl acrylate using DFT calculations with continuum solvation, the rate of reaction in various solvents correlated well with the dipole moment of the solvents; however, it was argued that a multipole approach was still needed[53]. Polar solvents still had a small effect on the rate if the charge transfer from the reactants to transition states, calculated using a Mulliken charge analysis[59], was low. Wong and Radom performed calculations using the self-consistent isodensity polarizable continuum model (SCIPCM)[55,60]. In the case of radicals with saturated substituents
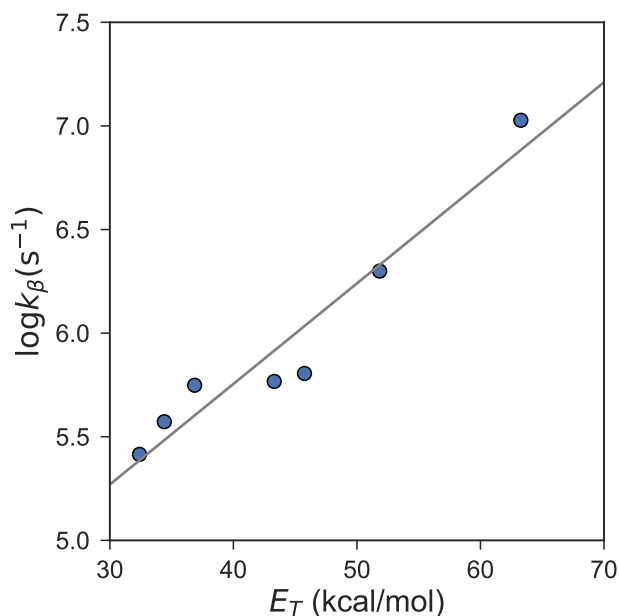
Figure 7: β-scission rates correlate with Dimroth-Reichardt parameter E_T. Data from[62]

adding to alkenes with saturated substituents, addition of any solvent increases the reaction barrier. Solvent decreases the barrier in the unsaturated case. The higher the dielectric constant of the solvent, the greater this effect. Finally, Garcia et al. investigated the addition of several radicals to methyl aminoacrylate with DFT and found that for an unspecified solvent, barriers increase with solvation for electrophilic radicals (phenyl and trifluoromethyl) and decrease for nucleophilic radicals (methoxymethyl and methyl)[61]. From these studies, it can be concluded that the chemical nature of the radical has a larger effect on the rates than the polarity of the solvents in this reaction family.

4.3 β-scission

The β-scission (reverse reaction of radical addition to multiple bond) of *tert*-butoxyl radicals was investigated by Weber and Fischer[63] using electron spin resonance to measure rates. They found that at 300 K, the rates in

solution were at least ten times larger than the gas phase rates. This result was explained by a transition state effect, where the transition state is more polar than the radical and is thus more stabilized by interactions with polar and polarizable solvents. Furthermore, the β-scission of cumyloxyl radicals measured using laser flash photolysis also showed a rate increase with increasing solvent polarity[64]. The same effect was found for alkyloxyl radicals[65]. Bietti et al. also confirmed this effect and found that the solvent Dimroth-Reichardt parameter (E_T) correlated well with the increase in rate[66], confirming earlier results by the Ingold group[62], see Figure 7. The E_T parameter represents the charge-transfer absorption of the solvent in pyridinium N-phenolbetaine and serves as a different measure of solvent polarity than the dielectric constant[67]. For example, methyl formamide has an extremely high dielectric constant but is of similar polarity to methanol as characterized by its E_T value.

It appears from these studies that the rates of β-scission reactions can be generalized to increase with some measure of solvent polarity such as E_T. However, since only reactions of cumyloxyl and alkyloxyl radicals have been investigated, and mostly in water, acetonitrile or mixtures of the two, it is perhaps dangerous to infer kinetic solvent effects for the entire reaction family.
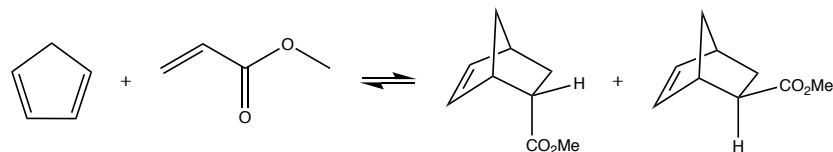
4.4 Diels-Alder

Figure 8: Example of Diels-Alder reaction of cyclopentadiene and methyl acrylate and possible product isomers

Like the other reaction families discussed thus far, the rates of Diels-Alder reactions in solution, in general, depend on both solute and solvent properties[68]. Breslow et al. described a large increase in rate of Diels-Alder reactions in water and in stereoselectivity between endo and exo products[69]. They explain the acceleration in terms of the reactant structures; the diene and dienophile engage in hydrophobic stacking. Experimental studies with

methanol show that it is indeed this hydrophobic effect, rather than a polarity effect, which increases the rate in water; the rates of some reactions actually decrease in methanol, which is unexpected.

Later, Ruiz-Lopez et al. studied Diels-Alder reactions of cyclopentadiene and methyl acrylate (Figure 8) using *ab initio* calculations[70]. They found that because the solvent's electric field changes the shape of the potential energy surface, a direct change in the overall reaction mechanism is seen with solvation. It is argued that only adding the solvation energy to the gas-phase energy is not sufficient to determine the reaction path in solution. However, they also maintain that continuum theory models are sufficient for capturing some specific interactions with solvents, such as hydrogen-bonding, since overall electrostatic effects will implicitly include these properties. Another simulation study on the reaction of methyl acrylate with cyclopentadiene was done by Sheehan and Sharratt using molecular dynamics[71]. The reaction was studied in both methanol and n-hexane. The result showed that the endo/exo selectivity of the reaction products is related to the difference in the solvated transition states' free energies. Further, the rates and selectivity were affected by properties of the solvent, such as their polarity and H-bonding ability. In methanol, the product was energetically favored as compared to in n-hexane; this effect was explained by the similarity in polarity between the product and methanol.

Soto-Delgado et al. studied the reaction of cyclopentadiene and methyl vinyl ketone in both water and methanol, using a combined QM/MM-MD approach[72]. The activation free-energy barrier in methanol is 2.1 kcal/mol higher than in water, which is within 0.1 kcal/mol from the experimental difference (a rate deceleration of 2 orders of magnitude). Again, the ability of the solvent and transition state to hydrogen bond, which is stronger and longer-lived in water than in methanol, contributes to this effect. Kiselev et al. compared reaction rates of 9-(hydroxymethyl)anthracene and 9,10-bis(hydroxymethyl)anthracene with maleic anhydride, N-ethylmaleimide and N- phenylmaleimide, in organic and water-1,4-dioxane cosolvents[73]. It was found that even those reactants which do not hydrogen-bond with water experienced reaction rate acceleration in water, depending on the structure of the diene. The organic cosolvents reduced the reaction rate, also depending on the polarity of the reactants.

These studies illustrate the importance of both polarity of reactants and hydrogen bonding ability in kinetic solvent effects of Diels-Alder reactions, and verify that continuum models and other computational methods can

capture both of these effects reasonably. Despite the success of these models, experimental studies were necessary to show the hydrophobic effect that is crucial in some cases. Additionally, merely adding solvation energies to those obtained in the gas-phase is not sufficient when the transition state geometries or shape of the potential energy surface change significantly in a solvent.
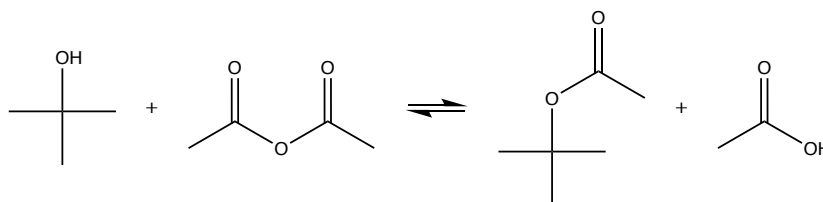
4.5   Acetylation

Figure 9:   Acetylation of tert-butyl alcohol by acetic anhydride

Xu et al. [74] theoretically investigated the catalyst-assisted acetylation of *tert*-butanol, displayed in Figure 9 with acetic anhydride in the gas phase and in three solvents. The optimized geometries and reaction energies were found with B3LYP/6-311++G(d,p) and B3LYP/6-31G(d), respectively, while solvation energies were found using PCM. The calculations showed that the reaction proceeds via a mechanism characterized by nucleophilic attack of the catalysis, and that this mechanism does not change, nor does the rate-limiting step, with solvent. Because polar solvents better solvate the reactants than the transition states or reaction intermediates, the reaction is less favorable in these solvents. Consequently, the reaction proceeds less favorably in going from gas, to carbon tetrachloride, to chloroform, and finally to dichloromethane, the most polar solvent of the group. These results are also supported by early experimental studies [75]. The investigations together illustrate that continuum solvation models can be sufficient to explain trends in solvation kinetics, and also that reaction rate can vary with solvent polarity alone.
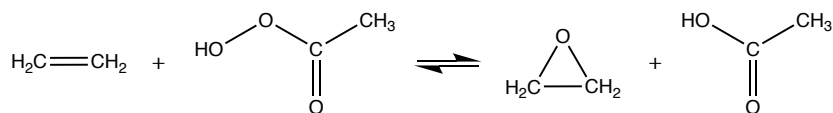
Figure 10: Epoxidation of ethane by peroxyacetic acid to form oxirane and acetic acid.

4.6 Epoxidation

The epoxidation of olefins (Figure 10) by hydrogen peroxide was studied both experimentally and with DFT by Berksessel and co-workers[25,76,77]. For these reactions, using fluorinated alcohols such as hexafluoroisopropanol (HFIP) accelerates the rate in relation to 1,4-dioxane[76,77]. From 0-4 molecules of HFIP were studied with the reactants quantum mechanically in the gas-phase, and then the whole system was treated with PCM[25]. Acetone was chosen as a model solvent for HFIP, because of its similar dielectric constant, with some additional considerations for cavitation. The activation enthalpies were shown to decrease with increasing number of HFIP molecules, while increasing contribution of entropy lead to the Gibbs free energy of activation reaching saturation with three or four HFIP molecules. The same theoretical study was done using methanol as a solvent, but increasing the number of methanol molecules had no influence. However, the activation barrier was reduced more with methanol than with HFIP. This result shows that methanol acts only as a polar solvent for the reaction, and explicit hydrogen-bonding with methanol does not affect the reaction rate, as it does with HFIP. While prior theoretical study by the Shaik group showed that fluorinated alcohols increased the epoxidation reaction rate[78], the studies by Berkessel explicitly showed the effect of multiple aggregates of the solvent molecules.

Later, Steenackers et al. experimentally studied the epoxidation of β - caryophyllene to caryopyllene oxide in aqueous H_2O_2, alcohols, nitrogen con-taining solvents, and furans (11 solvents in total)[79]. In all cases, the rate correlated extremely well with Abraham's hydrogen bonding parameters (R^2 = 0.97), and interestingly, not well at all with the dielectric constant (R^2 = 0.17), as shown in Figure 11. They further characterized solvent effect using ωB97XD/g-311++G(df,pd) and IEPCM. This computational investigation confirmed previous studies that the solvent stabilizes the O-O bond in H_2O_2 in the transition state structure via hydrogen bonding[79].

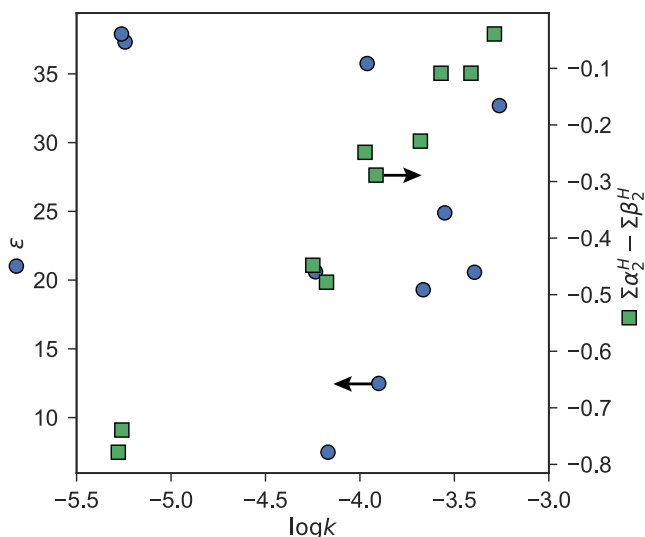These studies together show for some reaction families, hydrogen bonding

Figure 11: Differing solvent parameters versus the epoxidation rate of β-caryophyllene; data from[79]. Rate correlates well with the difference between solvent's hydrogen bond donor and acceptor characters, $\Sigma\alpha_2^H - \Sigma\beta_2^H$, but not with dielectric constant ϵ.

with solvent is more important than polarity to explain kinetic solvent effect. However, treating the solvent explicitly is occasionally necessary to deduce these effects, as was the case of HFIP vs. methanol[25,76,77].

4.7 Hydrolysis

Almerindo and Pliego studied the hydroylsis of formamide with ab initio calculations and PCM[80]. 1-4 explicit water molecules were considered, and both stepwise and concerted mechanisms were investigated. For the stepwise mechanism, the activation barrier increased by 4.6 kcal/mol with one water molecule (Figure 12a) and 11.0 kcal/mol with two water molecules (Figure 12b). Adding water molecules beyond two made the system entropically unfavorable. For the concerted mechanism, the solvation only increased the barrier by 6.4 kcal/mol with two water molecules (Figure 12c), indicating that the transition state is more stabilized by the solvent than in the stepwise mechanism. Additionally, the level of theory used for the calculations had a large effect on the barriers. The discrepancy caused by the level of theory
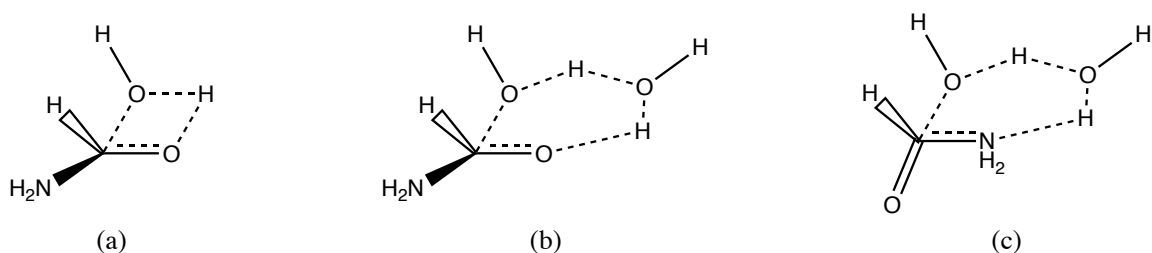
Figure 12: Mechanisms in the hydrolysis of formamide investigated in[80]. (a) Stepwise, one water molecule; (b) Stepwise, two-water catalyzed; (c) Concerted, two-water catalyzed

was larger than the difference between using geometries optimized in the liquid-phase, rather than geometries optimized in the gas phase and then modeled with PCM[80]. This study further confirms the usefulness of PCM for deducing both kinetic solvent effects and likely mechanistic pathways; however, care should be taken with the level of theory for quantum chemistry calculations.
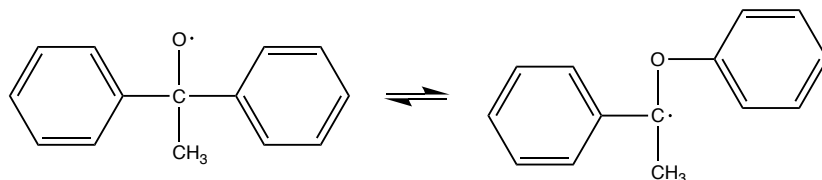
4.8   *O*-neophyl rearrangement

Figure 13:   *O*-neophyl rearrangement of 1,1-diphenylethoxyl radical

The *O*-neophyl rearrangement of two 1,1-diphenylethoxyl radicals, one of which is illustrated in Figure 13, was investigated with laser flash photolysis in five solvents by Bietti and Salamone[81]. For both radicals, the rate constant decreased with increasing solvent polarity. A linear correlation was found between the logarithm of the rearrangement rate constant and the Dimroth-Reichardt parameter E_T^N. Because E_T^N represents the solvent anion's solvating ability, the trend was explained in terms of the "decrease in the extent of negative charge on the oxygen atom on going from the starting

radical to the transition state."[81] This experimental study provides another example of solvent effect being deduced from a single solvent parameter.

5   Summary and Outlook

The above examples display that chemical reactivity can change drastically in different solvents, and that a diverse set of methods are used to determine this solvent effect. While some rates change systematically with a number of solvent polarity measures, it is not always clear which properties of the solvent and reactant structure will have an effect on the rates. Experimental data are only available for certain reactions in some reaction families, most extensively hydrogen abstraction. It is hard to generalize effects to a whole family of reactions without both experimental and theoretical data, and a variety of reactants and solvents tested, which would require a lot of experiments and/or calculations. Augmenting these data for reaction families beyond hydrogen abstraction would greatly benefit the kinetics community.

Further understanding can be driven by the experimental community by measuring reaction rates in strategically chosen sets of solvents; for example, solvents of different polarity that do not have the ability to hydrogen bond, or non-polar solvents that vary in molecular size and shape. These sets of solvents can potentially isolate different effects which cannot be explicitly seen computationally using polarizable continuum models. Computational efforts can be directed towards re-optimization of reactant and transition state geometries in solution in order to confirm that single-point energy calculations on gas phase geometries are enough. While increasing the level of theory of QM calculations is helpful, subtracting transition state and reactant energies in both phases will cancel some error introduced by the imperfect electronic structure calculations. Strategic collaboration between experimentalists and theorists are crucial to confirm and strengthen these conclusions about solvent effects.

Despite more complex effects, one generalization that can be made across the reaction families in section 4, is that computational methods including continuum solvation models have been successfully used in several of the studies to explain and predict solvent effects. Using a solvation model to calculate energies of geometries optimized in the gas-phase was shown to be sufficient in most cases, and is a promising approach to determining kinetic solvent effects going forward.

Understanding complex chemical systems requires detailed kinetic models, with each elementary reaction rate known or estimated. These models can be quite large; for example, a model for the liquid-phase oxidation of a biodiesel surrogate fuel blend contained 3,275 chemical reactions[2]. Due to the size of these models it is desirable to generate them automatically, but using quantum chemistry and transition state theory or direct dynamics to calculate thousands of liquid-phase reaction rates on-the-fly during mechanism generation would be computationally expensive. Jalan et al.[6] automated the estimation of solvation thermochemistry and diffusion limitations during automated mechanism generation, and manually modified some reaction rates on the basis of PCM calculations, to build solvent-sensitive models of tetralin oxidation. The next step is understanding how to systematically apply kinetic solvent effects to all the reactions, to improve accuracy and reduce human effort when building detailed kinetic models.

Correlating parameters with molecular structure features for the ultimate goal of predicting these parameters has proven effective for thermodynamic parameters[82], gas-phase reaction rates[83], and transition state geometries[84]. If shown that the properties of reacting molecules and solvent systematically affect reaction rates in liquids, such an approach can also be used to predict kinetic solvent effect. Machine learning provides a framework for parameter prediction based on molecular properties, using models fitted to known data. In addition to the above examples of chemical properties needed for detailed kinetic modeling, machine learning has been used to solve several problems in the domains of cheminformatics and bioinformatics[85–87].

The difficulties of such an approach are similar to the pitfalls of the methods described in this review; enough experimental or theoretical data must be generated to train such a model. One promising method for generating a large number of gas and liquid-phase reaction rates is automatic transition state calculations. For example, Bhoorasingh and West developed a machine learning algorithm for predicting key distances in the transition state for three families of reactions, allowing a good initial guess for the transition state geometry to be set up automatically[84]. This method has recently been integrated with a transition state theory calculator[88], providing a fully automated algorithm for calculating gas-phase reaction rates[89]. Integrating such methods with computational methods to calculate reaction rates in liquids, such as the continuum methods discussed in Section 3.2 and used in several of the discussed studies[25,53,55,74,79,80], could provide a systematic approach

to calculating many reaction rates in different solvents. This large volume of reaction rates could then be used to train a machine learning model to predict solvent effect from molecular properties. Generation of more accurate detailed kinetic models, which require many solution-phase rates, would then become possible.

References

[1] V. F. McNeill, J. L. Woo, D. D. Kim, A. N. Schwier, N. J. Wannell, A. J. Sumner, J. M. Barakat, Aqueous-Phase Secondary Organic Aerosol and Organosulfate Formation in Atmospheric Aerosols: A Modeling Study., Environ. Sci. Technol. 46 (15) (2012) 8075–8081. doi:10.1021/es3002986.

[2] A. Ben Amara, A. Nicolle, M. Alves-Fortunato, N. Jeuland, Toward Predictive Modeling of Petroleum and Biobased Fuel Stability: Kinetics of Methyl Oleate/ n-Dodecane Autoxidation, Energy Fuels 27 (10) (2013) 6125–6133. doi:10.1021/ef401360k.

[3] V. Thavasi, R. P. A. Bettens, L. P. Leong, Temperature and solvent effects on radical scavenging ability of phenols, J. Phys. Chem. A 113 (13) (2009) 3068–3077. doi:10.1021/jp806679v.

[4] H. Struebing, Z. Ganase, P. G. Karamertzanis, E. Siougkrou, P. Haycock, P. M. Piccione, A. Armstrong, A. Galindo, C. S. Adjiman, Computer-aided molecular design of solvents for accelerated reaction kinetics, Nat. Chem.doi:10.1038/nchem.1755.

[5] S. Rice, Diffusion-Controlled Reactions in Solution, in: C. Bamford, C. Tipper (Eds.), Compr. Chem. Kinet., Elsevier Pub. Co., Amsterdam, New York, 1985, Ch. 2, pp. 3–45.

[6] A. Jalan, R. H. West, W. H. Green, An Extensible Framework for Capturing Solvent Effects in Computer Generated Kinetic Models, J. Phys. Chem. B 117 (10) (2013) 2955–2970. doi:10.1021/jp310824h.

[7] F. F. Crim, Molecular reaction dynamics across the phases: similarities and differences, Faraday Discuss. 157 (2012) 9. doi:10.1039/c2fd20123b.

[8] Y. Liang, S. Liu, Y. Xia, Y. Li, Z.-X. Yu, Mechanism, regioselectivity, and the kinetics of phosphine-catalyzed [3+2] cycloaddition reactions of allenoates and electron-deficient alkenes, Chemistry – A European Journal 14 (14) (2008) 4361–4373. doi:10.1002/chem.200701725. URL http://dx.doi.org/10.1002/chem.200701725

[9] F. Briers, D. Chapman, E. Walters, The Influence of the Intensity of Illumination on the Velocity of Photochemical Changes. The Determination of the Mean Life of a Hypothetical Catalyst, J. Chem. Soc. 129 (1926) 562–569. doi:10.1039/JR9262900562.

[10] F. Briers, D. Chapman, The Influence of the Intensity of Illumination on the Velocity of the Photochemical Union of Bromine and Hydrogen, and the Determination of the Mean Life of a Postulated Catalyst., J. Chem. Soc. (1928) 1802–1811doi:10.1039/JR9280001802.

[11] E. T. Denisov, Liquid-Phase Reaction Rate Constants, Springer US, 2012. URL https://books.google.com/books?id=j8LeBwAAQBAJ

[12] H. W. Melville, The Photochemical Polymerization of Methyl Methacrylate Vapour, Proc. R. Soc. A Math. Phys. Eng. Sci. 163 (1937) 511–542. doi:10.1098/rspa.1937.0242.

[13] C. Swain, P. Bartlett, Rate Constants of the Steps in Addition Polymerization. II. Use of the Rotating-Sector Method on Liquid Vinyl Acetate, J. Am. Chem. Soc. 68 (11) (1946) 2381–2386. doi:10.1021/ja01215a072.

[14] A. Shepp, Rate of Recombination of Radicals. I. A General Sector Theory; A Correction to the Methyl Radical Recombination Rate, J. Chem. Phys. 24 (5) (1956) 939–943. doi:10.1063/1.1742719.

[15] D. Griller, K. U. Ingold, Free-Radical Clocks, Acc. Chem. Res. 13 (1980) 317–323. doi:10.1021/ar50153a004.

[16] D. Geske, A. Maki, Electrochemical Generation of Free Radicals and Their Study by Electron Spin Resonance Spectroscopy; the Nitrobenzene Anion Radical, J. Am. Chem. Soc. 82 (9) (1960) 2671–2676. doi:10.1021/ja01496a004.

[17] B. Roschek, K. A. Tallman, C. L. Rector, J. G. Gillmore, D. A. Pratt, C. Punta, N. A. Porter, Peroxyl radical clocks, J. Org. Chem. 71 (9) (2006) 3527–32. doi:10.1021/jo0601462.

[18] M. Jha, D. a. Pratt, Kinetic solvent effects on peroxyl radical reactions., Chem. Commun. (2008) 1252–1254doi:10.1039/b800369f.

[19] H. Eyring, H. Gershinowitz, C. E. Sun, The Absolute Rate of Homogeneous Atomic Reactions, J. Chem. Phys. 3 (12) (1935) 786. doi:10.1063/1.1749593.

[20] P. Hohenberg, W. Kohn, Inhomogeneous Electron Gas, Phys. Rev. 155 (1962) (1964) 864. doi:10.1103/PhysRev.136.B864.

[21] W. Kohn, L. J. Sham, Self-consistent equations including exchange and correlation effects, Phys. Rev. 385 (1951) (1965) 1133–1138. doi:10.1103/PhysRev.140.A1133.

[22] X. Xu, I. M. Alecu, D. G. Truhlar, How Well Can Modern Density Functionals Predict Internuclear Distances at Transition States ?, J. Chem. Theory Comput. 7 (2011) 1667–1676. doi:10.1021/ct2001057.

[23] A. J. Cohen, P. Mori-Sánchez, W. Yang, Insights into Current Limitations of Density Functional Theory, Science 321 (5890) (2008) 792–794. doi:10.1126/science.1158722.

[24] R. Arnaud, N. Bugaud, Role of polar and enthalpic effects in the addition of methyl radical to substituted alkenes: a density functional study including solvent effects, J. Am. Chem. Soc. 7863 (13) (1998) 5733–5740. doi:10.1021/ja973896p.

[25] A. Berkessel, J. A. Adrio, Dramatic Acceleration of Olefin Epoxidation in Fluorinated Alcohols: Activation of Hydrogen Peroxide by Multiple H-Bond Networks., J. Am. Chem. Soc. 128 (41) (2006) 13412–13420. doi:10.1021/ja0620181.

[26] A. Jalan, R. W. Ashcraft, R. H. West, W. H. Green, Predicting solvation energies for kinetic modeling, Annu. Rep. Prog. Chem., Sect. C: Phys. Chem. 106 (2010) 211–258. doi:10.1039/b811056p.

[27] B. Mennucci, R. Cammi (Eds.), Continuum Solvation Models in Chemical Physics: From Theory to Applications, John Wiley and Sons Ltd, The Atrium, Southern Gate, Chichester, West Sussex PO19 8SQ, England, 2007.

[28] A. Klamt, G. Schüürmann, COSMO: a new approach to dielectric screening in solvents with explicit expressions for the screening energy and its gradient, J. Chem. Soc. Perkin Trans. 2 2 (1993) 799–805. doi:10.1039/P29930000799.

[29] A. Klamt, Conductor-like Screening Model for Real Solvents: A New Approach to the Quantitative Calculation of Solvation Phenomena, J. Phys. Chem. 99 (1995) 2224–2235. doi:10.1021/j100007a062.

[30] A. Klamt, V. Jonas, T. Burger, J. C. Lohrenz, Refinement and Parametrization of COSMO-RS, J. Phys. Chem. A 102 (26) (1998) 5074–5085. doi:10.1021/jp980017s.

[31] J. R. Pliego, Shells theory of solvation and the long-range Born correction, Theor. Chem. Acc. 128 (3) (2011) 275–283. doi:10.1007/s00214-010-0844-1.

[32] A. V. Marenich, C. J. Cramer, D. G. Truhlar, Universal solvation model based on solute electron density and on a continuum model of the solvent defined by the bulk dielectric constant and atomic surface tensions., J. Phys. Chem. B 113 (18) (2009) 6378–6396. doi:10.1021/jp810292n.

[33] M. J. Frisch, G. W. Trucks, H. B. Schlegel, G. E. Scuseria, M. A. Robb, J. R. Cheeseman, G. Scalmani, V. Barone, B. Mennucci, G. A. Petersson, H. Nakatsuji, M. Caricato, X. Li, H. P. Hratchian, A. F. Izmaylov, J. Bloino, G. Zheng, J. L. Sonnenberg, M. Had, D. J. Fox, Gaussian 09, Revision D.01 (2009).

[34] S. Miertuš, E. Scrocco, J. Tomasi, Electrostatic interaction of a solute with a continuum. A direct utilization of ab initio molecular potentials for the prevision of solvent effects, Chem. Phys. 55 (1) (1981) 117–129. doi:10.1016/0301-0104(81)85090-2.

[35] K. Baldridge, A. Klamt, First principles implementation of solvent effects without outlying charge error, J. Chem. Phys. 106 (16) (1997) 6622. doi:10.1063/1.473662.

[36] A. Pomogaeva, D. M. Chipman, Hydration energy from a composite method for implicit representation of solvent, J. Chem. Theory Comput. 10 (1) (2014) 211–219. `doi:10.1021/ct400894j`.

[37] N. M. Silva, P. Deglmann, J. R. Pliego, CMIRS Solvation Model for Methanol: Parametrization, Testing, and Comparison with SMD, SM8, and COSMO-RS, J. Phys. Chem. B 120 (49) (2016) 12660–12668. `doi:10.1021/acs.jpcb.6b10249`.

[38] L. Valgimigli, J. Banks, Kinetic Solvent Effects on Hydroxylic Hydrogen Atom Abstractions Are Independent of the Nature of the Abstracting Radical. Two Extreme Tests Using Vitamin E and Phenol, J. Am. Chem. Soc. 117 (9) (1995) 9966–9971. `doi:10.1021/ja00145a005`.

[39] P. Das, M. Encinas, Reactions of tert-Butoxy Radicals with Phenols. Comparison with the Reactions of Carbonyl Triplets, J. Am. Chem. Soc. 103 (14) (1981) 4162–4166. `doi:10.1021/ja00404a030`.

[40] L. Valgimigli, K. U. Ingold, J. Lusztyk, Antioxidant Activities of Vitamin E Analogues in Water and a Kamlet-Taft beta-Value for Water, J. Am. Chem. Soc. 118 (15) (1996) 3545–3549. `doi:10.1021/ja954030r`.

[41] Z. Alfassi, R. Huie, P. Neta, Solvent Effects on the Rate Constants for Reaction of Trichloromethylperoxyl Radicals with Organic Reductants, J. Phys. Chem. 97 (28) (1993) 7253–7257. `doi:10.1021/j100130a022`.

[42] M. Foti, C. Daquino, C. Geraci, Electron-Transfer Reaction of Cinnamic Acids and Their Methyl Esters with the DPPH Radical in Alcoholic Solutions, J. Org. Chem. 69 (14) (2004) 2309–2314. `doi:10.1021/jo035758q`.

[43] D. Snelgrove, J. Lusztyk, Kinetic Solvent Effects on Hydrogen-Atom Abstractions: Reliable, Quantitative Predictions via a Single Empirical Equation, J. Am. Chem. Soc. 123 (3) (2001) 469–477. `doi:10.1021/ja002301e`.

[44] G. Litwinienko, K. U. Ingold, Abnormal solvent effects on hydrogen atom abstractions. 1. The reactions of phenols with 2,2-diphenyl-1-picrylhydrazyl (dpph*) in alcohols., J. Org. Chem. 68 (9) (2003) 3433–8. `doi:10.1021/jo026917t`.

[45] G. Litwinienko, K. U. Ingold, Abnormal solvent effects on hydrogen atom abstraction. 2. Resolution of the curcumin antioxidant controversy. The role of sequential proton loss electron transfer., J. Org. Chem. 69 (18) (2004) 5888–5896. `doi:10.1021/jo049254j`.

[46] G. Litwinienko, K. Ingold, Abnormal Solvent Effects on Hydrogen Atom Abstraction. 3. Novel Kinetics in Sequential Proton Loss Electron Transfer Chemistry, J. Org. Chem. 70 (22) (2005) 8982–8990. `doi:10.1021/jo051474p`.

[47] M. Nielsen, K. Ingold, Kinetic Solvent Effects on Proton and Hydrogen Atom Transfers from Phenols/ Similarities and Differences, J. Am. Chem. Soc. 128 (4) (2006) 1172–1182. `doi:10.1021/ja0548081`.

[48] M. Kamlet, R. Taft, The Solvatochromic Comparison Method. I. The beta-Scale of Solvent Hydrogen-Bond Acceptor (HBA) Basicities, J. Am. Chem. Soc. 98 (2) (1976) 377. `doi:10.1021/ja00418a009`.

[49] J. J. Warren, J. M. Mayer, Tuning of the thermochemical and kinetic properties of ascorbate by its local environment: solution chemistry and biochemical implications., J. Am. Chem. Soc. 132 (22) (2010) 7784–93. `doi:10.1021/ja102337n`.

[50] I. Sajenko, V. Pilepić, C. J. Brala, S. Ursić, Solvent dependence of the kinetic isotope effect in the reaction of ascorbate with the 2,2,6,6-tetramethylpiperidine-1-oxyl radical: tunnelling in a small molecule reaction., J. Phys. Chem. A 114 (10) (2010) 3423–3430. `doi:10.1021/jp911086n`.

[51] A. L. Koner, U. Pischel, W. M. Nau, Kinetic solvent effects on hydrogen abstraction reactions., Org. Lett. 9 (15) (2007) 2899–2902. `doi:10.1021/ol071165g`.

[52] J. Lalevée, X. Allonas, J. Fouassier, Reactivity of Carbon-Centered Radicals toward Acrylate Double Bonds: Relative Contribution of Polar vs. Enthalpy Effects, J. Phys. Chem. A 108 (19) (2004) 4326–4334. `doi:10.1021/jp037766g`.

[53] J. Lalevée, X. Allonas, J. P. Fouassier, D. Rinaldi, M. F. Ruiz Lopez, J. L. Rivail, Solvent effect on the radical addition reaction to double

bond: Experimental and quantum chemical investigations, Chem. Phys. Lett. 415 (2005) 202–205. `doi:10.1016/j.cplett.2005.08.137`.

[54] J. Lalevée, X. Allonas, J.-P. Fouassier, Addition of carbon-centered radicals to double bonds: influence of the alkene structure, J. Org. Chem. 70 (3) (2005) 814–819. `doi:10.1021/jo048381c`.

[55] M. W. Wong, L. Radom, Radical Addition to Alkenes: Further Assessment of Theoretical Procedures, J. Phys. Chem. A 102 (12) (1998) 2237–2245. `doi:10.1021/jp973427+`.

[56] H. Fischer, L. Radom, Factors Controlling the Addition of Carbon-Centered Radicals to Alkenes- An Experimental and Theoretical Perspective, Angew. Chemie Int. Ed. English 40 (2001) 1340–1371. `doi:10.1002/1521-3773(20010417)40:8<1340::AID-ANIE1340>3.0.CO;2-\#`.

[57] G. P. F. Wood, M. S. Gordon, L. Radom, D. M. Smith, Nature of Glycine and Its alpha-Carbon Radical in Aqueous Solution: A Theoretical Investigation, J. Chem. Theory Comput. 4 (10) (2008) 1788–1794. `doi:10.1021/ct8002942`.

[58] B. Chan, R. J. O'Reilly, C. J. Easton, L. Radom, Reactivities of Amino Acid Derivatives Toward Hydrogen Abstraction by Cl* and OH*, J. Org. Chem. 77 (2012) 9807–9812. `doi:10.1021/jo3021538`.

[59] R. S. Mulliken, Electronic Population Analysis on LCAO-MO Molecular Wave Functions. I, J. Chem. Phys. 23 (10) (1955) 1833. `doi:10.1063/1.1740588`.

[60] J. Tomasi, B. Mennucci, R. Cammi, Quantum mechanical continuum solvation models, Chem. Rev. 105 (8) (2005) 2999–3093. `doi:10.1021/cr9904009`.

[61] A. García, D. Domínguez, A. Navarro-Vázquez, Addition of carbon centered radicals to methyl 3-(methylamino)acrylate: The regioselectivity of radical addition to enamino esters, Comput. Theor. Chem. 979 (2012) 17–21. `doi:10.1016/j.comptc.2011.10.003`.

[62] D. V. Avila, U. Ingold, J. Lusztyk, Solvent Effects on the Competitive beta-Scission and Hydrogen Atom Abstraction Reactions of the Cumyloxyl Radical. Resolution of a Long-standing Problem, J. Am. Chem. Soc. 115 (2) (1993) 466–470. doi:10.1021/ja00055a015.

[63] M. Weber, H. Fischer, Absolute Rate Constants for the beta-Scission and Hydrogen Abstraction Reactions of the tert-Butoxyl Radical and for Several Radical Rearrangements: Evaluating Delayed Radical Formations by Time-Resolved Electron Spin Resonance, J. Am. Chem. Soc. 121 (32) (1999) 7381–7388. doi:10.1021/ja990837y.

[64] E. Baciocchi, M. Bietti, M. Salamone, S. Steenken, Spectral properties and absolute rate constants for beta-scission of ring-substituted cumyloxyl radicals. A laser flash photolysis study., J. Org. Chem. 67 (7) (2002) 2266–2270. doi:10.1021/jo0163041.

[65] M. Newcomb, P. Daublain, J. H. Horner, p-Nitrobenzenesulfenate Esters as Precursors for Laser Flash Photolysis Studies of Alkyl Radicals, J. Org. Chem. 67 (24) (2002) 8669–8671. doi:10.1021/jo026218g.

[66] M. Bietti, G. Gente, M. Salamone, Structural effects on the beta-scission reaction of tertiary arylcarbinyloxyl radicals. The role of alpha-cyclopropyl and alpha-cyclobutyl groups, J. Org. Chem. 70 (17) (2005) 6820–6826. doi:10.1021/jo050883i.

[67] C. Reichardt, Empirical Parameters of the Polarity of Solvents, Angew. Chemie Int. Ed. English 4 (1) (1965) 29. doi:10.1002/anie.196500291.

[68] R. Bini, C. Chiappe, V. Mestre, A rationalization of the solvent effect on the Diels-Alder reaction in ionic liquids using multiparameter linear solvation energy relationships, Org. Biomol. Chem. 6 (2008) 2522–2529. doi:10.1039/B802194E.

[69] R. Breslow, T. Guo, Diels-Alder Reactions in Nonaqueous Polar Solvents. Kinetic Effects of Chaotropic and Antichaotropic Agents and of beta-Cyclodextrin, J. Am. Chem. Soc. 110 (17) (1988) 5613–5617. doi:10.1021/ja00225a003.

[70] M. F. Ruiz-Lopez, X. Assfeld, J. I. Garcia, J. a. Mayoral, L. Salvatella, Solvent effects on the mechanism and selectivities of asymmetric Diels-Alder reactions, J. Am. Chem. Soc. 115 (19) (1993) 8780–8787. `doi:10.1021/ja00072a035`.

[71] M. E. Sheehan, P. N. Sharratt, Molecular dynamics methodology for the study of the solvent effects on a concentrated Diels-Alder reaction and the separation of the post-reaction mixture, Comput. Chem. Eng. 22 (1998) S27–S33. `doi:10.1016/S0098-1354(98)00035-0`.

[72] J. Soto-Delgado, R. A. Tapia, J. Torras, Multiscale Treatment for the Molecular Mechanism of a Diels-Alder Reaction in Solution: A QM/MM-MD Study, J. Chem. Theory Comput. 12 (10) (2016) 4735–4742. `doi:10.1021/acs.jctc.6b00772`.

[73] V. D. Kiselev, D. A. Kornilov, I. A. Sedov, A. I. Konovalov, Solvent Influence on the Diels-Alder Reaction Rates of 9-(Hydroxymethyl)anthracene and 9,10-Bis(hydroxymethyl)anthracene with Two Maleimides, Int. J. Chem. Kinet. 49 (1) (2017) 61–68. `doi:10.1002/kin.21057`.

[74] S. Xu, I. Held, B. Kempf, H. Mayr, W. Steglich, H. Zipse, The DMAP-catalyzed acetylation of alcohols–a mechanistic study (DMAP = 4-(dimethylamino)pyridine)., Chemistry 11 (16) (2005) 4751–4757. `doi:10.1002/chem.200500398`.

[75] A. Hassner, L. Krepski, V. Alexanian, Aminopyridines as acylation catalysts for tertiary alcohols, Tetrahedron 34 (1978) 2069–2076. `doi:10.1016/0040-4020(78)89005-X`.

[76] A. Berkessel, J. Adrio, Kinetic Studies of Olefin Epoxidation with Hydrogen Peroxide in 1,1,1,3,3,3,-Hexafluoro-2-propanol Reveal a Crucial Catalytic Role for Solvent Clusters, Adv. Synth. Catal. 346 (2004) 275–280. `doi:10.1002/adsc.200303222`.

[77] A. Berkessel, J. a. Adrio, D. Hüttenhain, J. M. Neudörfl, Unveiling the "booster effect" of fluorinated alcohol solvents: aggregation-induced conformational changes and cooperatively enhanced H-bonding, J. Am. Chem. Soc. 128 (26) (2006) 8421–8426. `doi:10.1021/ja0545463`.

[78] S. D. Visser, J. Kaneti, R. Neumann, S. Shaik, Fluorinated Alcohols Enable Olefin Epoxidation by H2O2: Template Catalysts, J. Org. Chem. 68 (7) (2003) 2903–2912. `doi:10.1021/jo034087t`.

[79] B. Steenackers, A. Neirinckx, L. DeCooman, I. Hermans, D. DeVos, The strained sesquiterpene beta-caryophyllene as a probe for the solvent-assisted epoxidation mechanism, ChemPhysChem 15 (2014) 966–973. `doi:10.1002/cphc.201300981`.

[80] G. Almerindo, J. Pliego, Ab initio investigation of the kinetics and mechanism of the neutral hydrolysis of formamide in aqueous solution, J. Braz. Chem. Soc. 18 (4) (2007) 696–702. `doi:10.1590/S0103-50532007000400005`.

[81] M. Bietti, M. Salamone, Solvent Effects on the O-Neophyl Rearrangement of 1,1-Diarylalkoxyl Radicals. A Laser Flash Photolysis Study, J. Org. Chem. 70 (25) (2005) 10603–10606. `doi:10.1021/jo0518755`.

[82] S. W. Benson, J. H. Buss, Additivity Rules for the Estimation of Molecular Properties. Thermodynamic Properties, J. Chem. Phys. 29 (3) (1958) 546. `doi:10.1063/1.1744539`.

[83] R. Sumathi, H. H. Carstensen, W. H. Green, Reaction rate prediction via group additivity part 1: H abstraction from alkanes by H and CH3, J. Phys. Chem. A 105 (28) (2001) 6910–6925. `doi:10.1021/jp010697q`.

[84] P. Bhoorasingh, R. West, Transition state geometry prediction using molecular group contributions, Phys. Chem. Chem. Phys. 17 (48) (2015) 32173–32182. `doi:10.1039/c5cp04706d`.

[85] L. Han, Y. Wang, S. H. Bryant, Developing and validating predictive decision tree models from mining chemical structural fingerprints and high–throughput screening data in PubChem, BMC Bioinformatics 9 (1) (2008) 401. `doi:10.1186/1471-2105-9-401`.

[86] D. Thornley, M. Zverev, S. Petridis, Machine learned regression for abductive DNA sequencing, Proc. - 6th Int. Conf. Mach. Learn. Appl. (ICMLA 2007) (2007) 254–259`doi:10.1109/ICMLA.2007.33`.

[87] Y. Hu, H. Cheng, Application of stochastic models in identification and apportionment of heavy metal pollution sources in the surface soils of

a large-scale region, Environ. Sci. Technol. 47 (8) (2013) 3752–3760. doi:10.1021/es304310k.

[88] J. W. Allen, W. H. Green, CanTherm: Open-source software for thermodynamics and kinetics. Included in: Reaction Mechanism Generator, v2.0.0 (2016).
URL http://reactionmechanismgenerator.github.io

[89] P. L. Bhoorasingh, B. L. Slakman, F. S. Khanshan, J. Y. Cain, R. H. West, Automated transition state theory calculations for high-throughput kinetics, J. Phys. Chem. A (2017) 10.1021/acs.jpca.7b07361doi:10.1021/acs.jpca.7b07361.